True-amplitude migration – the traveltime-based strategy

C. Vanelle, University of Kiel, M. Spinner, University of Karlsruhe, T. Hertweck, Fugro Seismic Imaging Limited, C. Jäger, University of Karlsruhe, D. Gajewski, University of Hamburg

This paper was prepared for presentation at the 9th International Congress of The Brazilian Geophysical Society, held in Salvador, Brazil, September 11–14, 2005.

Summary

True-amplitude migration of the Kirchhoff type is a task of high computational effort. A substantial part of this effort is spent on the calculation of proper weight functions to countermand the effect of geometrical spreading in the data. The generation of the weights is usually very time consuming. Also, the weights must be stored. Together with the traveltime tables which are needed for the stacking surfaces, this leads to large demands in computer storage in addition to the high requirements in CPU time. In this paper we propose a strategy to compute the weight functions directly from coarsely-gridded traveltimes. Together with a fast and accurate method for the interpolation of the traveltimes onto the required fine migration grid, this leads to considerable savings in CPU time as well as storage. Application to a complex synthetic data set demonstrates the high quality of our approach.

Introduction

True-amplitude prestack depth migration can be implemented as a specific form of the Kirchhoff type migration. In addition to providing a focused structural image of the subsurface, information on the reflection strength at the discontinuities in the medium is also available from such an image. This information can be used for AVO studies, which play a key role in reservoir characterisation, for example to estimate shear velocities without measuring shear waves, solely from PP data.

True-amplitude migration is carried out in terms of a weighted diffraction stack. For each subsurface point the seismic traces are stacked along the diffraction time surface for that point. Individual weight functions are applied during the stack to recover the reflection amplitude. The weights depend on dynamic wavefield properties which are usually computed by dynamic ray tracing together with the diffraction traveltimes. For a 3D experiment this results in a tremendous amount of auxiliary data which have to be generated and stored, thus making true-amplitude migration a task of high computational costs.

We suggest to reduce these costs with the traveltime-based strategy proposed in this paper. Here, the requirements in computer storage are significantly reduced, as the only auxiliary quantity required are the diffraction traveltimes, sampled on coarse grids. A fast and accurate interpolation is applied to obtain the stacking surfaces on the fine migration grid. As the weight functions can be directly expressed in terms of the interpolation coefficients and are computed on-the-fly during the migration, no additional quantities are required. Thus, the traveltime-based strategy leads to major savings in computer storage as well as in CPU time.

In the next section we will begin with an outline of the method. After a short introduction to true-amplitude migration, we will describe the traveltime-based strategy in detail, including the traveltime interpolation and the determination of the weight functions. We will then illustrate the method with a complex synthetic example. The resulting image as well as the reconstructed reflection coefficients demonstrate the high accuracy of the method. We will finalise this paper with our conclusions.

Method

For simplicity we will consider a 2.5D symmetry in this paper, where the medium does not vary in the direction perpendicular to the acquisition line. The method, however, is equally valid for the 3D case (see Vanelle, 2002).

Following the derivation of Schleicher et al. (1993), Martins et al. (1997) have shown that in 2.5D the true-amplitude migrated output $V(M)$ at the subsurface point M can be obtained from the weighted diffraction stack described by

$$V(M) = \frac{1}{\sqrt{2\pi}} \int\limits_A \mathrm{d}\xi \, W(\xi, M) \, D_t^{-1/2} U(\xi, t) \Big|_{t=\tau_D(\xi,M)} \, . \tag{1}$$

In Equation (1) the operator $D_t^{-1/2}$ denotes the Hilbert transform of the time half-derivative of the seismic data $U(\xi, t)$, where the data are assumed to consist of analytic traces. The integration is carried out over the aperture A which contains the considered trace positions that are represented by the so-called configuration parameter ξ. The stacking curve is the diffraction traveltime $t = \tau_D(\xi, M)$ for the depth point M, calculated in a previously determined macro-velocity model. The weight function $W(\xi, M)$ for the common-offset case

considered in this paper is given by

$$W(\xi,M) = \left|\frac{\cos\theta_S}{Q_{2,SM}}+\frac{\cos\theta_G}{Q_{2,GM}}\right| |Q_{2,SM}\,Q_{2,GM}|^{1/2} \times\sqrt{\frac{\sigma_{SM}+\sigma_{GM}}{v_S\,v_G}}\;\mathrm{e}^{-i\frac{\pi}{2}(\kappa_{SM}+\kappa_{GM})} \quad (2)$$

(Hanitzsch, 1997). Here, θ_S and θ_G are the emergence angle at the source ($S{=}S(\xi)$) and the incidence angle at the receiver ($G{=}G(\xi)$), respectively. The velocities at the source and receiver positions are v_S and v_G. The 2D scalar point source ray propagators $Q_{2,SM}$ and $Q_{2,GM}$ are closely related to the in-plane geometrical spreading between the source or receiver and the image point M. The quantities σ_{SM} and σ_{GM} denote the out-of-plane spreadings, and, finally, the KMAH indices κ_{SM} and κ_{GM} account for the number of caustics along the rays.

While the quantities σ and $\cos\theta$ can be obtained from kinematic ray tracing, dynamic ray tracing is required for the determination of the Q_2. In the traveltime-based approach we express Q_2 as well as σ and $\cos\theta$ in terms of first- and second-order traveltime derivatives. Thus, dynamic ray tracing is not required as these values are obtained from traveltimes. The traveltime derivatives are also used for the interpolation onto the fine migration grid. As all quantities are computed on the fly, only coarsely-gridded traveltimes need to be stored (in contrast to the conventional approach, where we must store the Q_2, σ, and $\cos\theta$ in addition to the traveltimes), thus a considerable amount of storage and computational time can be saved. We will now describe the traveltime interpolation method which will lead to the mentioned replacement of Q_2, σ, and $\cos\theta$ by traveltime derivatives.

We use the following expression for the traveltime from a source S at the position $\mathbf{s}$ to a subsurface point M at the position $\mathbf{m}$ (Vanelle and Gajewski, 2002):

$$\begin{aligned} T^2(\mathbf{s},\mathbf{m}) &= (T_1-\mathbf{p}_1\Delta\mathbf{s}+\mathbf{q}_1\Delta\mathbf{m})^2 \\ &\quad -2\,T_1\,\Delta\mathbf{s}\cdot\underline{\mathbf{N}}_1\Delta\mathbf{m} \\ &\quad -T_1\,(\Delta\mathbf{s}\cdot\underline{\mathbf{S}}_1\Delta\mathbf{s}-\Delta\mathbf{m}\cdot\underline{\mathbf{G}}_1\Delta\mathbf{m}) \quad (3)\end{aligned}$$

The traveltime T_1 is that from a source at $\mathbf{s}_0$ to a subsurface point at $\mathbf{m}_0$. We will refer to the combinations of $(\mathbf{s}_0,\mathbf{m}_0)$ as the expansion points that are represented by the coarse grid. The slowness vectors $\mathbf{p}_1$ and $\mathbf{q}_1$ are the first-order traveltime derivatives at the source and subsurface point, respectively. The three matrices

$$S_{1_{ij}} = -\frac{\partial^2 T}{\partial s_i\,\partial s_j}\;, \qquad G_{1_{ij}} = \frac{\partial^2 T}{\partial m_i\,\partial m_j}\;,$$
$$N_{1_{ij}} = -\frac{\partial^2 T}{\partial s_i\,\partial m_j}\;,$$

are the second-order derivatives of the traveltime. Correspondingly, we use

$$\begin{aligned} T^2(\mathbf{g},\mathbf{m}) &= (T_2-\mathbf{p}_2\Delta\mathbf{g}+\mathbf{q}_2\Delta\mathbf{m})^2 \\ &\quad -2\,T_2\,\Delta\mathbf{g}\cdot\underline{\mathbf{N}}_2\Delta\mathbf{m} \\ &\quad -T_2\,(\Delta\mathbf{g}\cdot\underline{\mathbf{S}}_2\Delta\mathbf{g}-\Delta\mathbf{m}\cdot\underline{\mathbf{G}}_2\Delta\mathbf{m}) \quad (4)\end{aligned}$$

for the traveltime from a receiver G at the position $\mathbf{g}$ to a subsurface point. Since the traveltimes are in any event required for the stacking surface, we assume that these are available and sampled on coarse grids. As described in Vanelle and Gajewski (2002), all coefficients in Equations (3) and (4) can be determined from the traveltime tables. The coefficients can then be applied for the interpolation of the traveltimes onto the fine migration grid. If only first-arrival traveltimes are given, the KMAH indices are zero. If later arrivals are considered, it is convenient to generate the tables for the individual arrivals with an algorithm that outputs them sorted by KMAH, e.g., with the wavefront-oriented ray tracing technique by Coman and Gajewski (2001).

The relations between the quantities that appear in the weight function (2) and the coefficients of Equations (3) and (4) are

$$\begin{aligned} Q_{2,SM} &= \frac{v_S\,p_{1_z}\;v_M\,q_{1_z}}{N_{1_{xx}}}\,, & Q_{2,GM} &= \frac{v_G\,p_{2_z}\;v_M\,q_{2_z}}{N_{2_{xx}}}\,, \\ \sigma_{SM} &= \frac{1}{N_{1_{yy}}}\,, & \sigma_{GM} &= \frac{1}{N_{2_{yy}}}\,, \\ \cos\theta_S &= v_S\,p_{1_z}\,, & \cos\theta_G &= v_G\,p_{2_z} \end{aligned} \quad (5)$$

(Vanelle, 2002). With them, we can express the weight (2) by

$$W(\xi,M) = \left|\frac{N_{1_{xx}}}{q_{1_z}}+\frac{N_{2_{xx}}}{q_{2_z}}\right| \left|\frac{q_{1_z}}{N_{1_{xx}}}\,\frac{q_{2_z}}{N_{2_{xx}}}\right|^{1/2} \times\sqrt{\frac{1}{N_{1_{yy}}}+\frac{1}{N_{2_{yy}}}}\;\sqrt{p_{1_z}\,p_{2_z}} \times\mathrm{e}^{-i\frac{\pi}{2}(\kappa_{SM}+\kappa_{GM})}\;. \quad (6)$$

In the following section we will apply the traveltime interpolation (3) and (4) and the weight functions (6) to a synthetic data set.

Example

We have applied the method to a complex velocity model displayed in Figure 1. Ray synthetic seismograms were obtained from a 2.5D ray modelling package resulting in 60,000 traces which cover an offset range from 0 to 1980 m. Figure 2 shows the zero-offset section. The required traveltime tables were computed with a 3D finite differences eikonal solver in a smoothed version of the model and stored on a 100 m grid. These were the only input data used for the computation of the true-amplitude weight functions. Only primary reflections and

first arrivals were considered during the migration.

The depth migrated section is shown in Figure 3. The smile-like migration artifacts are mainly caused by abrupt amplitude variations along reflectors and missing diffracted energy at the pinch-outs in the model (cf. the zero-offset section in Figure 2). They stem from the ray tracing program applied to generate the synthetic seismograms. These inconsistencies in the input data would lead to artifacts in any migrated section of this data set, regardless of the migration algorithm, and are not a problem of our method in particular.

The common-image gather displayed in Figure 4 was extracted at a distance of 2.6 km. The events are flat and the AVO behaviour is altogether smooth. Some scattering of the amplitudes can be observed at the deeper reflectors. This is again caused by the missing diffraction events at the pinch-outs and the discontinuous amplitudes in the input data already discussed above.

In order to verify the quality of the recovered reflectivity, we have chosen the top reflector which is horizontal at the distance of 2.6 km. This makes it possible to compare the results to the analytic solution because the incidence angle is available. Also, the velocity in the uppermost layer is constant which enables us to compare our results to those from a migration with the analytic form of Equation (2) for the constant velocity case. We have, therefore, picked the amplitudes from the image gather in Figure 4 and from the corresponding gather obtained with the constant velocity weight. Both are displayed together with the analytic result in Figure 5. As the differences between our results and the analytic one as well as the results from the constant velocity migration are practically negligible, this reflects the high accuracy of the migration weights obtained from traveltimes.

The traveltime-based migration took about the same time that was required for a purely kinematic migration (i.e., no weight function is applied at all) when the traveltimes are interpolated linearly. In that case the grid spacing must be chosen smaller than is possible with the hyperbolic interpolation of traveltimes used for this study. Since a dynamic ray tracing routine was not available for a direct comparison, we have tested the computational efficiency of our method for a model where we could analytically compute the dynamic wavefield properties required for the weights. The comparison showed that application of our method leads to savings in computational time of a factor of five. At the same time the computer storage could be reduced by a factor of 100. We expect that the gain in efficiency that can be achieved in three dimensions will be a multiple of these numbers.

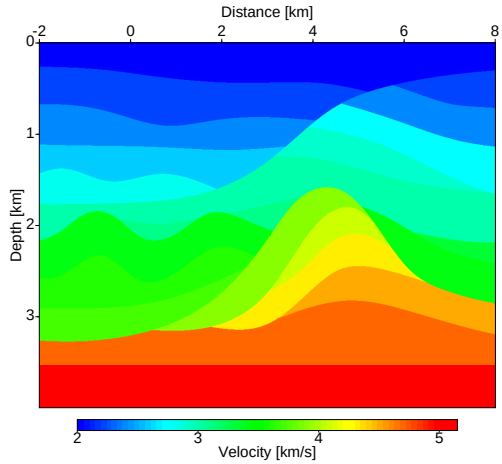

Fig. 1: The velocity model.

Conclusions

By applying the traveltime-based strategy for true-amplitude migration we can obtain a dynamically correct depth migrated image at the computational cost of a kinematic migration. In comparison to using the standard weight functions (e.g., obtained from dynamic ray tracing) the computational speed of our method is five times higher and the storage requirements are a factor of 100 less in the case of a 2.5D medium. We expect that the computational efficiency concerning both CPU time and storage will be significantly enhanced in the 3D case. We have also shown that the reflection coefficients can be recovered with the same accuracy as for standard weights. Thus, the traveltime-based approach is a promising strategy, especially in view of a 3D implementation that we are currently working on.

Acknowledgements

We thank the members of the Applied Geophysics Groups in Hamburg and Karlsruhe for continuous discussions. This work was partially supported by the sponsors of the Wave Inversion Technology (WIT) consortium and the German Research Foundation (DFG, grants Va 207/3-1 and Ga 350/10-2).

References

Coman, R. and Gajewski, D., 2001. Estimation of multivalued arrivals in 3-D models using wavefront ray tracing. In: Expanded Abstracts, p. MODP2.5. Soc. Expl. Geophys.

Hanitzsch, C., 1997. Comparison of weights in prestack amplitude-preserving depth migration. Geophysics, 62, 1812–1816.

Martins, J. L., Schleicher, J., Tygel, M., and Santos, L., 1997. 2.5-D true-amplitude migration and demigration. J. Seis. Expl., 6, 159–180.

Schleicher, J., Tygel, M., and Hubral, P., 1993. 3D true-amplitude finite-offset migration. Geophysics, 58, 1112–1126.

Vanelle, C., 2002. Traveltime-based true-amplitude migration. Ph.D. thesis, University of Hamburg.

Vanelle, C. and Gajewski, D., 2002. Second-order interpolation of traveltimes. Geophys. Prosp., 50, 73–83.

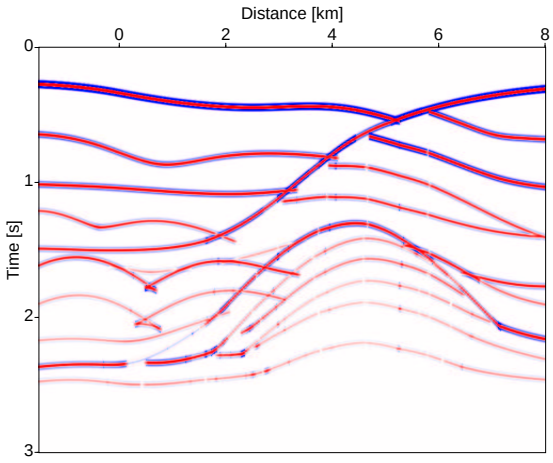

Fig. 2: The zero-offset section obtained by ray modelling.

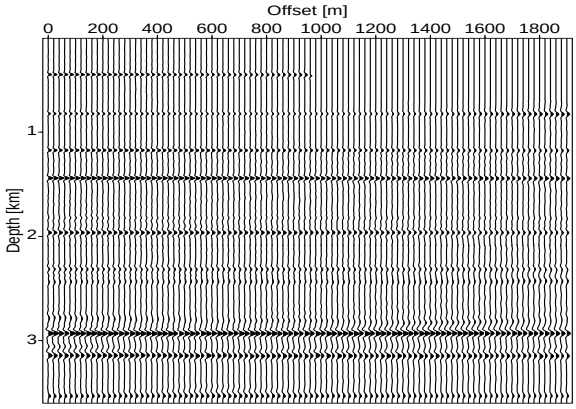

Fig. 4: Common-image gather taken at a distance of 2.6 km. A mute was applied to the larger offsets at shallower depths to avoid the pulse stretch. The events are flat and the AVO behaviour is altogether smooth. Some scattering of the amplitudes can be observed at the deeper reflectors. This is caused by the missing diffraction events in the input data discussed in the text.

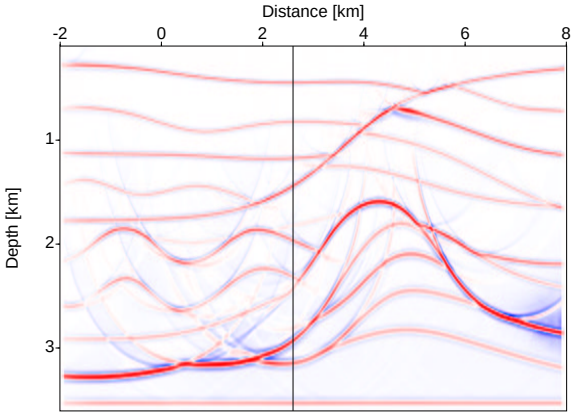

Fig. 3: The true-amplitude depth migrated section. The weight functions were obtained using coarsely-gridded traveltime tables only, no dynamic ray tracing had to be applied. The computational time required to perform the true-amplitude migration was comparable to a kinematic migration. The vertical line indicates the position where the common-image gather in Figure 4 is taken.

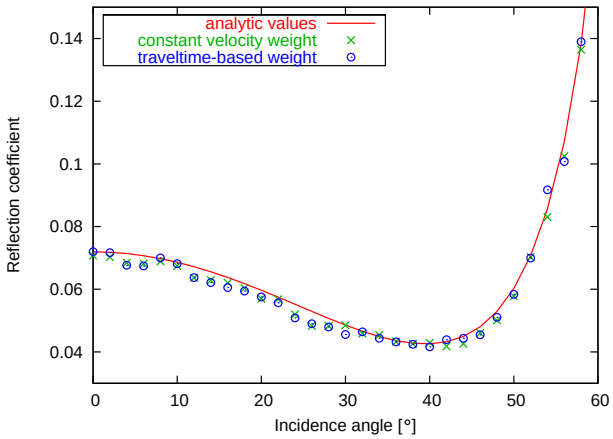

Fig. 5: Reconstructed reflection coefficients picked from the image gather in Figure 4 (blue circles) and from a migration with a constant velocity (analytic) weight funtion (green crosses). Both are compared to the exact solution (red line). The differences are negligible, which reflects the high accuracy of our method.